Plasmonic Meta-atoms and Metasurfaces

Nina Meinzer, William L. Barnes and Ian R. Hooper

Department of Physics and Astronomy,
University of Exeter,
Stocker Road,
Exeter,
EX4 4QL,
United Kingdom

Abstract

Despite the extraordinary degree of interest in optical metamaterials in recent years the hoped-for devices and applications have, in large part, yet to emerge, and it is becoming clear that the first generation of metamaterial-based devices will more likely arise from their two-dimensional equivalents, metasurfaces. In this review we describe the recent progress made in the area of metasurfaces formed from plasmonic meta-atoms. In particular we approach the subject from the perspective of the fundamental excitations supported by the meta-atoms and the interactions between them. We also identify some areas ripe for future research, and indicate likely avenues for future device development.

Introduction

The natural starting point in a review about plasmonic meta-atoms and metasurfaces is to explain what we mean by these terms. Whilst we will leave a more detailed description of plasmonic meta-atoms until the section of this review on the building blocks of metasurfaces and their interactions, in essence we can simply consider them to be sub-wavelength metallic elements that exhibit effective electric and/or magnetic polarisabilities defined by both their material properties and their geometry. In the context of this review these effective polarisabilities arise from the plasmonic modes supported by metallic nanostructures, which allow the electric and magnetic fields associated with light to be confined to deeply sub-wavelength regions[1].

These meta-atom building blocks can then be arranged into periodic arrays to form one-dimensional chains, two-dimensional metasurfaces, and three-dimensional metamaterials (see Fig. 1), where the electromagnetic response of the whole arises from the individual properties, or the collective responses, of the constituent elements[2]. The appeal of these meta-systems lies in their ability to exhibit electromagnetic properties that are not available from naturally occurring materials, such as the well-documented negative refractive index[3,4] that caused such an upsurge in metamaterial research at the turn of the millennium, they also open up opportunities in nonlinear photonics[5–9] and imaging[10].

Unfortunately, even after the enormous efforts expended on 3D optical metamaterials research over the last decade, many of the hoped-for applications and devices still seem a long way off. This can mostly be attributed to absorptive losses inherent in plasmonic

metals at optical frequencies[11], and to the challenges in fabricating complex three-dimensional geometries at the nanoscale[12]. Whilst absorptive losses will always be present in metal-based metamaterial systems (though there is increasing interest in all-dielectric approaches[13,14]), it is natural to ask whether meta-systems of reduced dimensionality, which are far simpler to fabricate, might be a more productive avenue.

In this article we will review the advances made over recent years in both the physics and the applications of plasmonic metasurfaces. This review is in three parts: we begin by looking at plasmonic particles (meta-atoms) and their interactions. We then explore the collective excitations that arrays of such meta-atoms support before moving on to discuss a specific application, that of phase-gradient metasurfaces (surfaces that allow the phase and amplitude of scattered wavefronts to be spatially tailored over sub-wavelength scales). We conclude this review with an outlook concerning directions for future research.

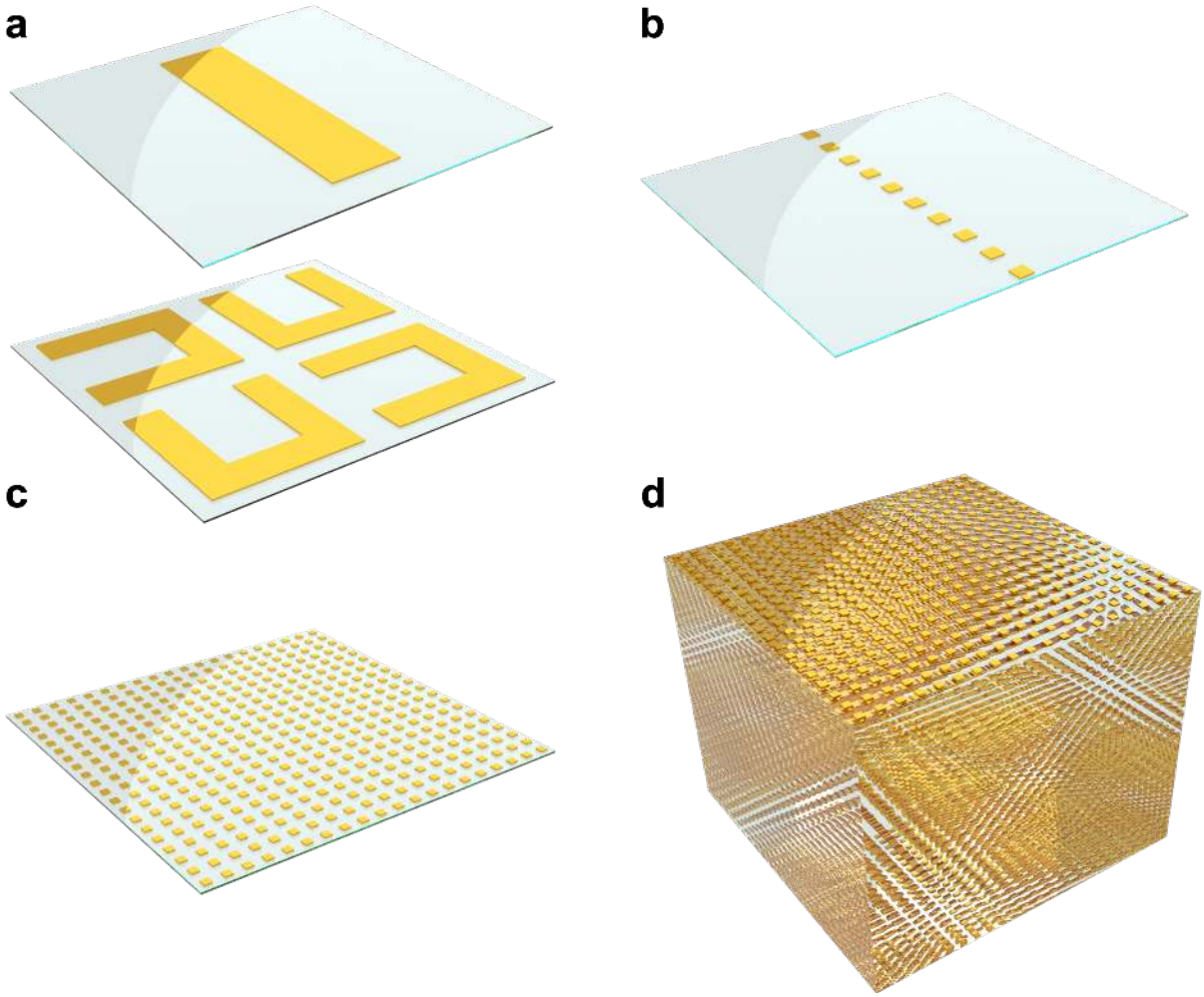

Fig. 1: **From meta-atoms to metamaterials.** (a) Schematic representation of two possible building blocks of meta-systems: a meta-atom in the form of a plasmonic nanorod, and a collection of split-ring resonators that form a meta-molecule. (b-d) Representations of a 1D chain, a 2D metasurface, and a 3D metamaterial made from plasmonic meta-atoms.

Plasmonic meta-atoms and their interactions

Plasmonic metamaterials are based on meta-atoms made from metallic nanostructures whose optical response is governed by the particle plasmon resonances they support.

When an electric field is applied to a metallic particle the conduction electrons are displaced from their equilibrium position with respect to the core ions, causing a polarisation of the particle and a depolarising field that acts as a restoring force. In a time-varying external field this collective motion can be described as a Lorentzian oscillator, with its characteristic peak in the displacement amplitude (polarisability) around the resonance frequency accompanied by a π phase shift over the spectral width of the resonance. It is this resonant phase behaviour that is the basis of many phase-gradient metasurface devices, which will be discussed in detail in a later section.

For very small particles the electric field penetrates the whole volume of the particle, polarising it completely, thereby resulting in a dipolar response whose resonant frequency depends on the material the particle is made of, its shape, and its dielectric environment[15]. However, when the particle dimensions are larger, retardation becomes important, furthermore, when the size is more than twice the skin depth the electric field acts primarily on the surface electrons giving rise to higher-order multipole resonances. The result is that, for these larger particles, the plasmon resonance is even more sensitive to the size and shape of the particle. Exact analytical solutions for the case of spherical particles were derived by Mie[16], and exist for ellipsoids[17] (Fig. 2a) for which the resonant frequency further depends on the orientation of the particle, relative to the driving field.

Another simple meta-atom, similar to spheroids, is that of a metal nanorod with sub-wavelength dimensions (Fig. 2b), which, to a first approximation, acts as a dipole antenna that supports a half-wavelength resonance along its principal axis[18]. One can use this basic antenna element to build up more complex meta-atoms (see Box 1). Instead of antennae one can also design metamaterials based on inverse structures, i.e. sub-wavelength apertures in a metallic sheet[19–21] and utilise Babinet's principle[22,23] or extraordinary transmission[24] based on surface-plasmon excitation.

A variety of fabrication techniques have been used to produce plasmonic meta-atoms and metasurfaces, and a range of structures from the literature are shown in Fig. 2 (details of their fabrication can be found in the references in the caption). There is also a review article that discusses the fabrication of such structures in detail[25].

Box1: From plasmonic antennae to meta-atoms

In addition to the fundamental half-wavelength eigenmode, a sufficiently long nanorod antenna supports higher-order modes, even when folded into more complex shapes. Such deformations have two main effects: firstly, the resonance frequency is shifted due to modified dipolar interactions between the ends of the antenna, creating an additional degree of tunability. Furthermore, folding the rod changes the symmetry of the antenna and as a result formerly dark modes may couple to incident light for appropriate directions of the incident electric field. For example, folding a nanorod along its middle creates a V-shaped antenna (Fig. 2c and Fig. B1) where one can describe the two lowest-order eigenmodes in terms of symmetric and anti-symmetric charge density distributions. These modes can be excited by light polarised along the symmetry axis and orthogonal to the symmetry axis of the structure respectively.

Additionally the current distribution of the anti-symmetric resonance resembles a

circulating ring current, inducing an out-of plane magnetic moment, which provides a magnetic-response of the antenna, even at optical frequencies. Such magnetic responses are necessary for negative refractive index materials[113–115], which require both the permittivity and the permeability of the material to be negative. However, the magnetic moment for a V-shaped antenna is weak and it is more common to use C- or U-shaped antennae[116] (Fig. 2e and f), which are usually referred to as split-ring resonators (SRRs)[117–120]. Ring currents can also be generated by stacking two rods, separated by a thin dielectric spacer, along the propagation direction of the incident light. In this configuration, retardation effects allow the anti-symmetric mode to be excited in the rods; the charge distribution forms a current loop, inducing a magnetic moment in the sample plane. To achieve a negative-index material these sandwich structures are combined with long wires to give a metallic response, resulting in the well-known fishnet structure[121] (Fig. 2h).

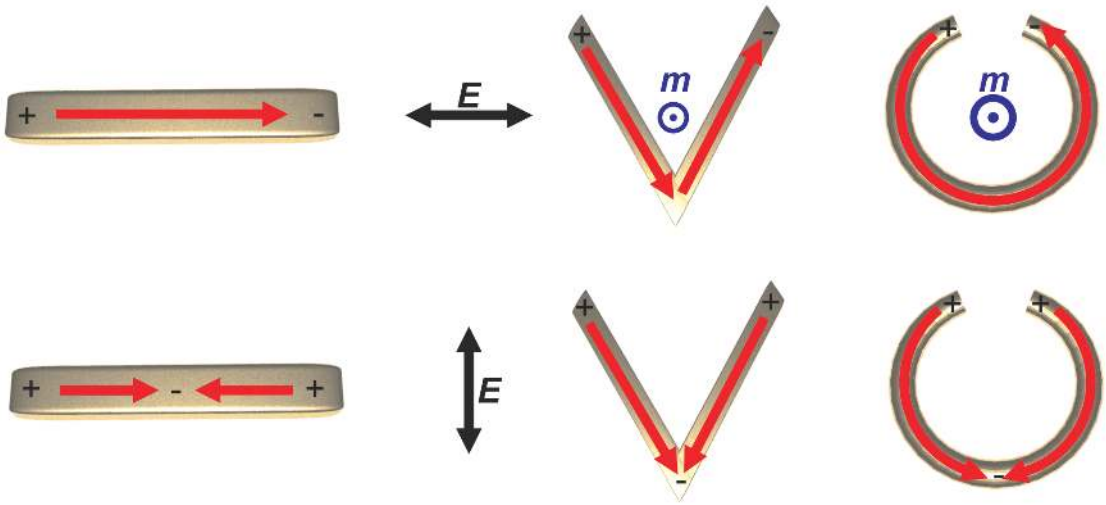

Fig. B1: Transition from a simple rod antenna into a V-shaped antenna and a split-ring resonator. The charge distributions of the lowest-order eigenmodes are shown, along with the resulting electric (red) and magnetic (blue) dipole moments, and the polarisation directions required to excite the modes.

When two meta-atoms are brought into close proximity interesting things start to happen. One can describe two near-field coupled meta-atoms (antennae) as coupled dipoles that exhibit hybridisation, i.e. the creation of symmetric and anti-symmetric modes according to the relative direction of the two dipoles[26,27]. For the anti-symmetric mode there is no net dipole moment, light normally incident on the plane containing both elements cannot couple to this mode (it is considered a dark mode) unless the symmetry is broken, e.g. by introducing a geometrical asymmetry (for an example see Fig. 2g). The resulting grey mode exhibits a very small net dipole moment and couples only weakly to optical fields. Consequently, the associated resonance exhibits low radiative losses and thus a narrow linewidth, making it interesting for sensing applications or for coupling to excitonic materials. The occurrence of such modes in plasmonic structures is extensively discussed in other reviews[28,29]. Further, the changes to the resonance position and width associated with mode-hybridisation depend strongly on the separation between the two particles[30,31], due in part to the attenuation of the near-fields with distance[32,33] and in part due to interference arising because of retardation, i.e. the finite speed of light[30,31,34].

In the case of magnetic meta-atoms, such as split-ring resonators, we have to consider both electric and magnetic dipole moments if we are to understand their interaction properly[35]. Whether electric or magnetic coupling mechanisms dominate depends strongly on the relative orientation of the resonators and on their orientation with respect to the incident field.

Going beyond a simple point dipole picture one can elicit an entirely different response from meta-atoms. By suitable structural design one can arrange for spatially and spectrally overlapped electric and magnetic field components to couple[36], enabling near fields to take on a chiral character[36–39]. (Fig. 2d shows an example of chiral meta-atoms), which can ultimately result in chiroptical far-field effects like optical activity or circular dichroism far stronger than anything observed in natural materials[40–42]. These effects, in turn, enable one to twist and control the polarisation of light in an unprecedented way, making chiral metamaterials interesting for applications such as ultrathin wave retarders. Furthermore, owing to their ability to efficiently couple to circularly polarised light as well as to molecules, such chiral metamaterials have recently been studied as an intermediary to enhance the usually rather weak interaction of light with chiral molecules[43].

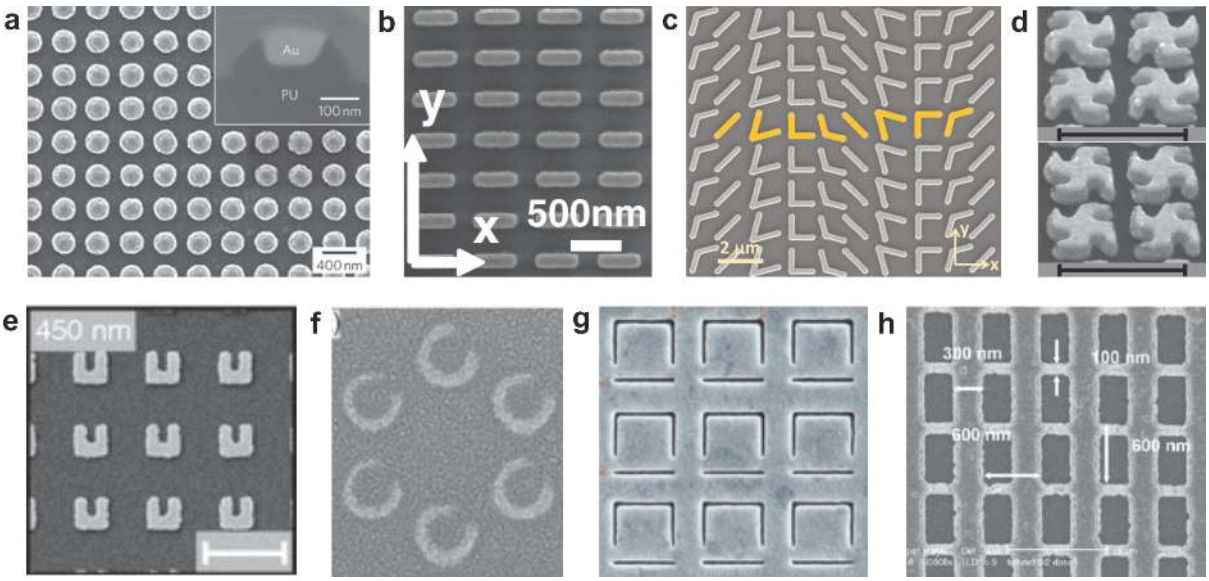

Fig. 2: Meta-atoms and metasurface fabrication techniques. (a) Nanodiscs fabricated by template-stripping. (b) Rod antennae fabricated by nanoimprint. (c) A metasurface composed of different V-shaped antennae fabricated by electron-beam lithography (EBL). (d) Double-layer right-handed (top) and left-handed (bottom) gammadions forming a chiral metamaterial fabricated by EBL; scale bar is 500 nm. (e) Split-ring resonators fabricated by EBL; scale bar is 500 nm. (f) SRR with an inner diameter of 108 nm and an outer diameter of 188 nm. The structures were fabricated by nanosphere lithography. (g) Inverse asymmetric SRR fabricated by ion-beam milling 25 nm wide slits into a gold film resulting in a 495 nm x 495 nm meta-atom, which is arranged on a square lattice with a period of 731 nm. (h) Double fishnet structure fabricated by nanoimprint. [Figures reproduced from: (a)[62], (b)[49], (c)[80], (d)[108], (e)[34], (f)[109], (g)[110], (h)[111]].

Collective Excitations

Qualitatively different things happen if we consider periodic arrays of meta-atoms. The plasmonic modes supported by an individual meta-atom will be modified by the presence of other members of the array, and two kinds of change to the response may occur. Firstly, the proximity of nearest neighbours will lead to a change in the field distribution around a particle, thereby altering its polarisability in a similar manner to that described above for pairs of particles. Secondly, for arrays of appropriate period, the possibility exists for coherent interactions between many particles, from which new collective modes emerge.

We may distinguish three regimes for 2D arrays of plasmonic meta-atoms: in the first regime the meta-atom separation is of order the resonance wavelength. Here, diffractive far-field interactions between the meta-atoms of the array may constructively interfere leading to collective modes known as surface lattice resonances (SLRs). Magneto-inductive interactions are also possible[44]. In the second regime the meta-atom separation is less than the resonance wavelength but meta-atoms are still sufficiently well separated that near-field mediated interactions are small; the phase-graded metasurfaces discussed in the next section fit into this category. In the third regime the meta-atom separation is small when compared with the resonance wavelength, and near-field interactions become very important. An example is the Dirac-like plasmons in honeycomb arrays of metallic nanoparticles in which the meta-atom separation is an order of magnitude less than the resonance wavelength[45].

When the array period is of order the wavelength of the particle resonance, neighbouring particles may interact coherently. More specifically, light scattered by one element in the array may act to drive a neighbouring particle in phase with the incident light. These surface lattice resonances involve a collectively scattered field that comprises components produced by scattering from all members of the array – with the array period such that all the contributions accumulate in phase. Such SLRs were predicted in the context of plasmonically resonant particles nearly 30 years ago but were not fully observed until relatively recently[46–48], see Fig. 3. SLRs can be spectrally much sharper than the plasmon resonance associated with individual particles from which they originate (see Fig 3a), they also offer an interesting way to couple light from nearby emitters to radiation, and as a consequence, they are being actively explored for potential in light emitting devices such as LEDs[49,50] and for light harvesting[51]. Intriguingly, making the unit cell more complex, e.g. by placing two meta-atoms in each unit cell, may open up additional design opportunities for surface lattice resonances; initial reports are encouraging[46]. A topic of much debate recently in the plasmonics community has been that of bright and dark modes[52], i.e. those modes that are dipole-allowed in terms of coupling to far-field radiation (bright) and those that are (largely) dipole forbidden (dark). As discussed above in the context of meta-atoms, the introduction of asymmetries may also allow the dark modes of arrays to be turned grey[53,54].

Array structures that support plasmon modes may also be harnessed to make lasers[55]. Early work in this area investigated the use of an array of gold nanoparticles as the feedback element in a polymer laser[56], however the gold particles were simply used as scatterers with no direct use being made of their plasmonic properties – indeed, the

emission wavelength of ~490 nm lies in the inter-band absorption region for the gold particles used. Lasing has more recently been reported for gold nanoparticle arrays covered by a dye-doped polymer film for which the emission wavelength was ~900 nm[57], well away from the inter-band absorption of gold. Very recently the role of the band structure in such array-based lasers has been explored[55], see Fig 3b. To probe more clearly the concept of lasing using such structures the interplay of the gain bandwidth and the plasmon resonances needs to be explored. It is interesting to note that hole arrays in a gold film have been successfully coupled to InGaAs gain layers to produce plasmonic hole array lasers[58], with clear evidence of a correlation between linewidth and lasing threshold as a function of pump power[59], as required to demonstrate lasing[60]. The subject of individual nanolasers is the topic for one of the other reviews in this special issue (review article by Martin Hill and Malte Gather, Nat Photon, XXX, XXXX-XXXX (2014))[61].

Since metasurfaces are frequently probed optically using normal-incidence illumination it is the collective modes based on electric dipole moments in the plane of the array that are typically involved, collective excitations involving out-of-plane electric dipole moments have received much less attention. Optical illumination away from normal incidence is a natural approach to probe such modes, and has been used to demonstrate the existence of collective modes involving out-of-plane dipole moments in far-field coupled arrays of gold nanorods made by template stripping[62]. An alternative way of exciting out-of-plane resonances is to use electrons: when an electron passes close to a metallic nanoparticle the time-varying current associated with the electron motion (as seen by the nanoparticle) may couple to the field associated with the plasmon mode; out-of-plane dipole moments are easily coupled to in this way[63,64]. This technique of electron energy loss spectroscopy (EELS) is likely to find increasing use in the study of metal-based metasurfaces, it is already proving a powerful tool in the field of quantum plasmonics[65].

Out-of-plane dipole moments are also important in more deeply sub-wavelength arrays, and remarkable effects have been predicted for honeycomb arrays of meta-atoms whose period is an order of magnitude less than the resonance wavelength, especially the emergence of Dirac-like collective plasmons[45,66]. These collective tuneable excitations are predicted to exhibit some of the unique features of electrons in graphene, such as non-trivial Berry phase[67,68] and the absence of backscattering from impurities[69]. More recently further interesting effects have been predicted, including birefringence arising from interactions between meta-atoms in a 3D cubic lattice, something one would normally consider to behave isotropically[70]. These fascinating properties are based upon the dipolar interactions between the meta-atoms.

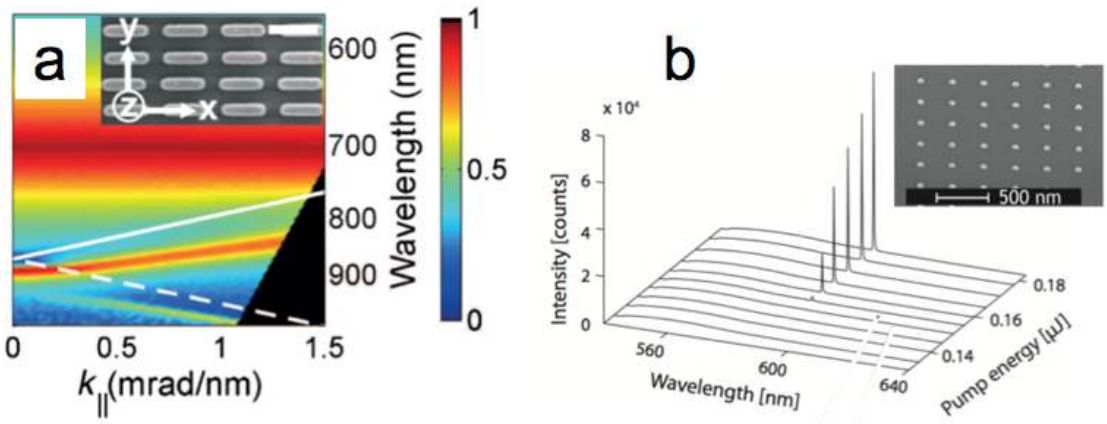

Fig 3: Plasmonic nanoparticle arrays. The figure shows two of the phenomena associated with nanoparticle arrays; on the left (a) experimental data portray a surface lattice resonance, on the right (b) lasing associated with a periodic array is also portrayed with the aid of experimental data. (a) Measured extinction as a function of wavelength and in-plane wave-vector from an array of gold nanorods (inset, scale bar is 500 nm). The spectra show a broad dispersion-less peak (red) at around 700 nm, this is the particle resonance associated with individual nanorods, and has a Q-value of < 10. The much sharper extinction peak (red), Q > 30, that tracks the diffraction edge (white solid and dashed lines) is the collective mode, the surface lattice resonance (reproduced from[54]). (b) Emission spectra from a band-edge plasmonic lattice comprising a square array of silver nanoparticles (inset) covered by a rhodamine 6G doped layer. As the pump power is increased the lasing output rises rapidly. (Data are from[55]).

Phase-gradient metasurfaces

In the regime in which the meta-atom separation is less than the resonance wavelength, but meta-atoms are still sufficiently well separated that near-field mediated interactions are small, one can spatially vary the shape of the meta-atoms in order to specifically tailor the phase and amplitude of the transmitted scattered wavefronts. Such systems have been termed phase-gradient metasurfaces and, in contrast to the typically bulky optical phase-control devices such as waveplates and spatial light modulators that rely on wave propagation through refractive media, they allow phase control across a distance that is very significantly sub-wavelength. However, whilst this is a relatively new area of research in the nanophotonics community, similar concepts have been employed in the RF and microwave antenna communities since the early 20th century, notably in the context of phased array antennas for RADAR applications[71]. We can distinguish between two main types of meta-atom elements suitable for phase-gradient metasurfaces: those in which the phase change is wavelength-dependent and results from the Lorentzian nature of the plasmonic resonance, and those which solely rely upon the geometry of the meta-atom to produce broadband phase changes (see Box 2). However, beyond these particle-based meta-atom designs, there are a family of more complex phase control metasurfaces that we will not discuss here in detail, but which should be noted. For example, Pors *et al.*[72,73] used gap surface plasmon (GSP) geometries consisting of metallic patches spaced above a metallic ground plane, and demonstrated their applicability for wavefront control in the optical and near-IR frequency regimes. These GSP geometries utilise the same concepts as reflectarrays at radio frequencies, which rely upon a coupling between the antenna and its image source in the back plane in order to generate a full 2π phase coverage (as is required for full

phase control of light)[74]. Such systems only operate in reflection, but do allow much higher scattering efficiencies (>80%), than the particle-based systems described here (~20%). There have also been several variations of reflectarray and meta-atom based phase-gradient metasurfaces such as arrays of H-shaped elements above a ground plane that have been used to modify the coupling of free space radiation into surface modes[75]; and 3-layer fishnet structures[76], arrays of crossed nanorods[77], and V-shaped cuts in thin metal films[78,79].

Box 2: Phase-gradient metasurface elements

The Lorentzian character of the plasmonic resonances supported by V-shaped nano-antennae allows control of the phase of the scattered light over a π phase range by modifying the geometry. However, for full phase control one requires 2π phase-coverage, and Yu *et al*. realised that, for linearly polarised incident light, a 90-degree rotation of the V-shaped antenna allows the remaining π range to be accessed in the cross-polarised scattered waves[80,112,122]. One can also use arbitrary orientations of C-shaped antennae for independent control of phase and amplitude as demonstrated by Liu *et al*.[116]. Here, the opening angle determines the phase of the scattered wavefronts and the orientation determines their amplitude. Due to the resonant basis of the phase-control these designs are inherently narrow-band. However, it should be noted that the bandwidth can be markedly improved in reflectarray geometries (in which the resonant antennae are spaced from a reflecting ground plane) due to a counterbalancing of the dispersion of the antenna with that of the multiple reflections within the spacer layer[72,74].

Broadband phase-control of scattered wavefronts can be achieved using a simple nanorod design, but only for circularly polarised incident light[83]. The phase-control is a direct result of the conversion of a proportion of the incident light into scattered wavefronts of the opposite handedness, and can be described in the context of an acquisition of Pancharatnam-Berry phase[123–125]. Whilst the amplitude results from the resonant character and can be controlled through a modification of the antenna length, the phase of the scattered wavefronts depends only upon the orientation of the nanorod. This can be readily understood by considering the transmission of circularly polarised light through a wire grid polariser: the transmitted light consists of a linear combination of equal-amplitude left- and right-handed circular polarisation components, and any rotation of the polariser results in a phase-change in the helically converted component that depends only upon the orientation of the polariser.

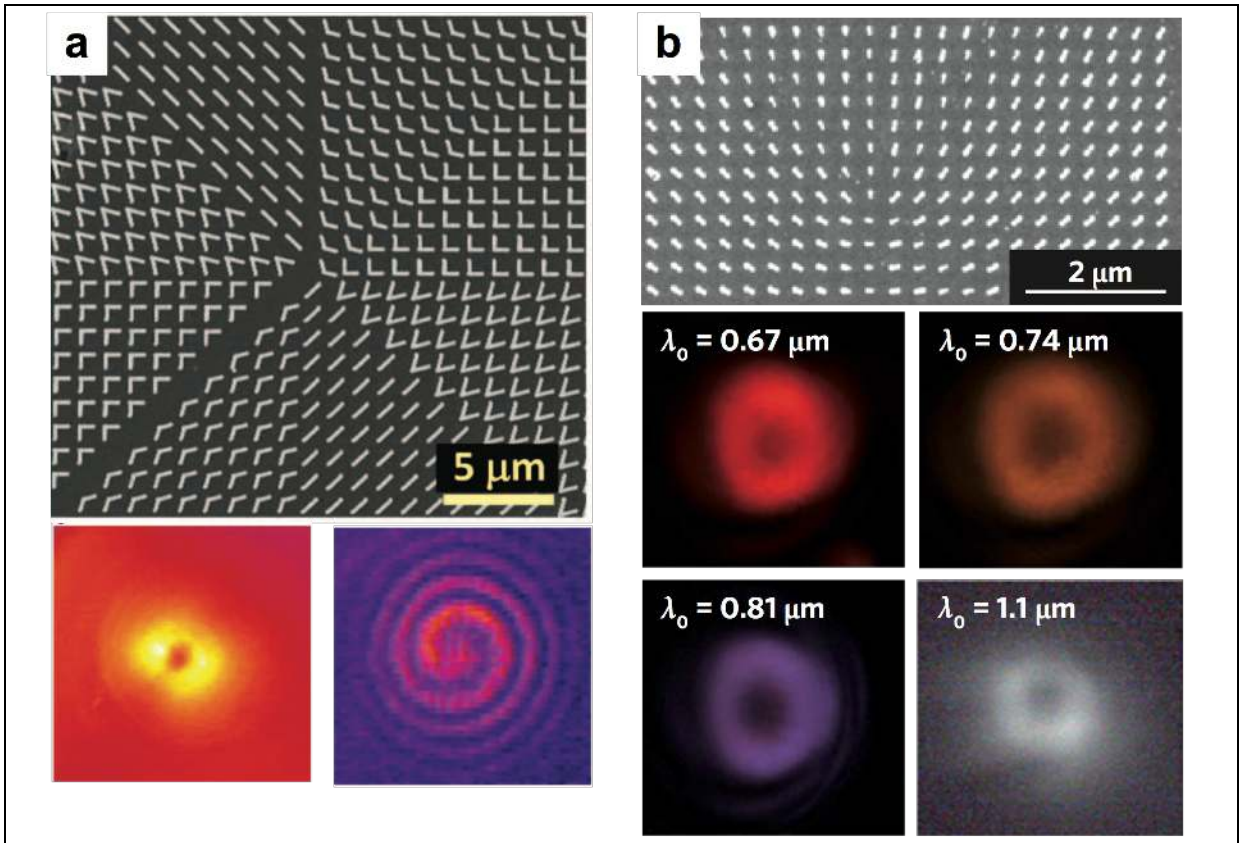

Fig. B2: Vortex beam generators formed from two types of phase-gradient metasurface elements. (a) Top: SEM image of a phase-graded metasurface formed of V-shaped nano-antennae designed to generate an optical vortex beam with a single twist of the wavefronts per wavelength. Bottom: The measured intensity distribution of the generated vortex beam, and the spiral interferogram, indicative of a first order vortex beam[80]. (b) Top: SEM image of a similar phase-graded metasurface formed of nanorods. The response can be broadband since the phase jumps originate from polarisation changes generated by the geometry. Bottom: The measured intensity distributions of the generated vortex beams for different wavelengths demonstrating the broadband nature of the device[83].

Once one has designed the individual meta-atoms that generate the required phase and amplitude control, the next step is to spatially pattern them. The first demonstration of a phase-gradient metasurface was undertaken by Yu *et al*.[80], who used V-shaped antennae to produce a 1D linear phase-gradient in the scattered cross-polarised fields as a function of distance along a metasurface using a periodic patterning of 8 different V-shaped antenna designs (see figure 4a). They found that all of the power was redirected out of the normally refracted direction, and described their results using "generalised laws of reflection and refraction". It should also be noted Larouche and Smith[81] have argued that the "generalised laws of reflection and refraction" are equivalent to diffraction from a blazed phase grating[82] arising due to the repeating period of 2π in the linear phase gradient.

By extending the patterning into 2D, one can design more complex optical components. In their original phase-graded metasurface paper Yu *et al*.[80] also described an optical vortex beam generator using the same V-shaped elements as in their linearly graded design, and Huang *et al*.[83] have subsequently demonstrated a broadband equivalent (see Fig. B2). Optical vortex beams exhibit corkscrew shaped wavefronts and possess orbital angular momentum[84,85], with the order of the vortex being given by the number of

twists in the wavefront per wavelength. The devices shown in Fig. B2 generate 1st order vortex beams requiring metasurfaces that provide a 2π phase variation in the azimuthal direction. In the broadband design this was simply achieved by rotating the rectangular nano-antennae around a central defect. The generated beams can be characterised by either measuring their intensity profiles, which exhibit a null in the centre of the beam for 1st order vortices, or by interfering the vortex beam with a co-propagating Gaussian beam, resulting in a spiral interferogram.

Other 2D phase-graded metasurface devices have also been developed such as quarter-wave plates[86] (Fig. 4b), and planar lenses and axicons[87,88]. The quarter-wave plate metasurface consists of the same unit cell as the linear phase-graded metasurface, but with alternate rows offset by a quarter of a period. The cross-polarised scattered wavefronts generated by the alternate rows are 90 degrees out of phase with each other resulting in circularly polarised scattered light. Lens and axicon designs utilise radial distributions of phase controlling elements in order to achieve their function.

Perhaps the most striking examples of phase control in traditional refractive optics are produced by holograms, and Huang *et al*. have demonstrated phase-graded metasurface holograms with full 3D image reconstruction[89] (figure 4c). The required phase map was calculated using a computer generated holography (CGH) algorithm[90] similar to that used for holographic images using spatial light modulators. A metasurface to generate the required phase profile was subsequently designed and fabricated, and the holographic image was observed upon illumination with circularly polarised light. Similar holographic concepts have also been used to develop phase-graded metasurfaces that can act as different optical devices depending upon the polarisation of the incident light[91], and have also been implemented in the Babinet-inverse structure of nano-antenna holes cut into a metal film[79]. More detailed descriptions of phase-gradient devices can be found in the review article by Yu *et al*.[92].

In addition to allowing the development of optical devices, phase-graded metasurfaces can also display striking evidence of fundamental physical phenomena - an example of which is the Photonic Spin Hall Effect (PSHE)[93,94]. The PSHE is the photonic analogue of the regular spin Hall effect, in which spin-orbit coupling of electrons generates a transverse motion, resulting in an accumulation of spin on either side of a current carrying wire[95]. In the case of the PSHE, when a light wave propagates along a curved trajectory a geometric polarisation rotation is induced in order to conserve polarisation in the direction transverse to its altered direction. This leads to an accumulation of oppositely circularly polarised light on either side of the beam. Yin *et al*.[94] realised that, since phase-graded metasurfaces are able to induce large changes in the propagation direction of a beam over a very sub-wavelength distance, they should exhibit large PSHEs. They successfully demonstrated this by measuring the polarisation state of the extraordinary beam generated by a linearly phase-graded metasurface formed from V-shaped antennae, and observed the expected accumulation of left and right handed circularly polarised light in the direction transverse to the direction of the phase-grading (see figure 4d).

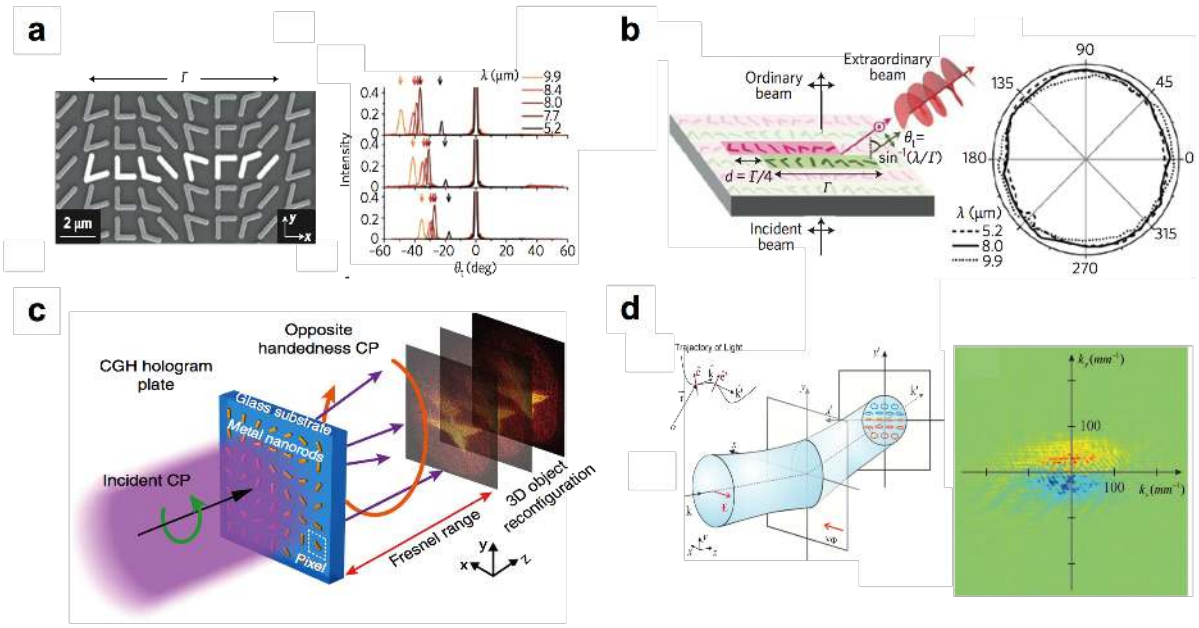

Fig. 4: Examples of phase-gradient metasurface devices. (a) Left: SEM image of a metasurface that generates a linear phase gradient via an array of V-shaped gold meta-atoms. The repeating unit cell is highlighted and has a period of Γ=11 μm. The phase gradient mimics the effects of a blazed phase grating. Right: Measured far-field intensity profiles. The intensity of the zeroth-order and diffracted (anomalously refracted) beams generated from a normally incident plane wave are shown for metasurfaces with Γ=13 (upper), 15 (middle) and 17 μm (lower). The deflection angle of the scattered beam depends upon the wavelength and lattice spacing, and agrees with predictions obtained using the generalised laws of refraction (arrows). (b) Left: Schematic showing a metasurface quarter-wave plate. The unit cell consists of two subunits (pink and green) offset by d=Γ/4. Upon illumination with normally incident linearly polarised light, a circularly polarised diffracted beam is generated due to the phase-shifted wavefronts originating from the subunits. Right: The polarisation state of the diffracted beam for different wavelengths determined by measuring the intensity as a function of the angle of a linear polariser placed in its path. (c) Schematic demonstrating how a phase-graded metasurface can generate holograms. Each meta-atom acts as a phase modifying pixel that, upon illumination with circularly polarised light, generates the required local phase profile for holographic reconstruction in the transmitted beam of opposite helicity. (d) Left: Upon propagation through an appropriate metasurface the rapid phase retardation generates a strong spin-orbit interaction leading to an accumulation of circularly polarised components in the transverse directions of the beam. Right: Observation of the PSHE via measurement of the helicity of the anomalously refracted beam from a linearly phase-graded metasurface formed from V-shaped elements. Red and blue represents right and left circular polarisations respectively. [Figures reproduced from: (a)&(b)[112], (c)[89], (d)[94]]

Outlook

Whilst we can expect research into 3D optical metamaterials to continue apace, it is clear that metasurfaces offer an accessible avenue for progress without some of the fabrication challenges of their three-dimensional brethren. Thus it is likely that the first generation of practical optical devices will utilise metasurface implementations.

Even though phase-gradient metasurfaces composed of plasmonic antennae have only recently emerged as an active area of research, their potential as a means to produce wavefront-shaping devices has already been demonstrated by the successful implementation of waveplates, vortex-beam generators, lenses and holograms (as discussed above). Many of these elements are essential for state-of-the-art imaging

systems and could be further miniaturised and tailor-made utilising the concepts of metasurfaces. We expect that future work in this area will be increasingly dedicated to the development of device applications. We also note the recent progress in the development of dielectric resonators at optical frequencies and their potential use in phase-gradient metasurfaces. It is hoped that, by eliminating the losses inherent in plasmonic resonances, these dielectric structures will enable devices with increased efficiency[14,96,97].

There is also the question of whether non-periodic metasurfaces will demonstrate phenomena that periodic structures do not. Despite some interesting initial work – the area is reviewed in [98] – this is largely an open question. Thus far there appears to be little if any work whose focus is that of harnessing such random structures for metamaterials, although there are some fascinating phenomena that may have potential. For example coherent emission from random structures in the form of random lasers is an active area of research [99,100]. Indeed, lasing based on metasurfaces is a new area of research for which experiment needs to catch up with theory; as an example coherent emission from zero-order, non-diffracting structures, as envisaged in the lasing-spaser concept[101] has yet to be demonstrated.

Higher levels of functionality for metasurfaces, such as switching, are desirable, especially for applications. One approach would be to combine magnetic and plasmonic functionalities[102], or to harness nonlinearlities[5,103], another is to exploit the interaction of particle plasmons with quantum emitters. The plasmonic meta-atom/quantum emitter interaction is an emerging area of research[104], for example with regard to strong coupling of excitonic materials both with single antennae[105] and with collective plasmon modes[106], and also with regard to the potential for enhancing the performance of applications like LEDs and solar cells. However, despite substantial effort dedicated to exploring the interplay between (sub-diffractive) metamaterials and active materials, there are still open questions that warrant further investigation. In this context it might also be interesting to explore the emission of light from emitters coupled to Dirac-like plasmons in the honeycomb metallic nanoparticle arrays discussed above. The unique predicted properties of these arrays remain to be experimentally tested and verified. We anticipate that electron-loss spectroscopy combined with advances in fabrication techniques such as directed self-assembly[107] will bring these ideas within the reach of experimental demonstration.

It is clear that there is a great deal of potential in this area that is yet to be realised and that research into optical metasurfaces will continue to be a very active and exciting field in the coming years, both in terms of fundamental scientific research and, increasingly, in the development of practical devices.

Correspondence and requests for materials should be addressed to William Barnes w.l.barnes@exeter.ac.uk

Acknowledgements

The authors would like to acknowledge the support of the EPSRC through the programme grant EP/I034548/1 (QUEST), and the support of the Leverhulme Trust.

References

1. Gramotnev, D. K. & Bozhevolnyi, S. I. Plasmonics beyond the diffraction limit. *Nat. Photonics* **4,** 83–91 (2010).

2. Cai, W. & Shalaev, V. M. *Optical Metamaterials*. (Springer, 2010).

3. Veselago, V. G. The electrodynamics of substances with simultaneously negative values of epsilon and mu. *Sov. Phys. Uspekhi* **10,** 509–514 (1968).

4. Smith, D. R., Pendry, J. B. & Wiltshire, M. C. K. Metamaterials and negative refractive index. *Science (80-.).* **305,** 788–792 (2004).

5. Kauranen, M. & Zayats, A. V. Nonlinear plasmonics. *Nat. Photonics* **6,** 737–748 (2012).

6. Metzger, B., Schumacher, T., Hentschel, M., Lippitz, M. & Giessen, H. Third harmonic mechanism in complex plasmonic Fano structures. *ACS Photonics* **1,** 471–476 (2014).

7. Czaplicki, R. *et al.* Enhancement of second harmonic generation from metallic nanoparticles by passive elemenst. *Phys. Rev. Lett.* **110,** 093902 (2013).

8. Chen, S. *et al.* Symmetry-selective third-harmonic generation from plasmonic metacrystals. *Phys. Rev. Lett.* **113,** 033901 (2014).

9. Linden, S. *et al.* Collective effects in second-harmonic generation from split ring resonator arrays. *Phys. Rev. Lett.* **109,** 015502 (2012).

10. Lu, D. & Liu, Z. Hyperlenses and metalenses for far-field super-resolution imaging. *Nat. Commun.* **3,** 1205 (2012).

11. Boltasseva, A. & Atwater, H. A. Low-loss plasmonic metamaterials. *Science (80-.).* **331,** 290–291 (2011).

12. Soukoulis, C. M. & Wegener, M. Past achievements and future challenges in the development of three-dimensional photonic metamaterials. *Nat. Photonics* **5,** 523–530 (2011).

13. Ginn, J. C. *et al.* Realizing Optical Magnetism from Dielectric Metamaterials. *Phys. Rev. Lett.* **108,** 097402 (2012).

14. Moitra, P. *et al.* Realization of an all-dielectric zero-index optical metamaterial. *Nat. Photonics* **7,** 791–795 (2013).

15. Kelly, K. L., Coronado, E., Zhao, L. L. & Schatz, G. C. The optical properties of metal nanoparticles: The influence of size, shape, and dielectric environment. *J. Phys. Chem. B* **107,** 668–677 (2003).

16. Mie, G. Beiträge zur Optik trüber Medien, speziell kolloidaler Metallösungen. *Ann. Phys.* **25,** 377–445 (1908).

17. Asano, S. & Yamamoto, G. Light scattering by a spheroidal particle. *Appl. Opt.* **14,** 29–49 (1975).

18. Novotny, L. Effective Wavelength Scaling for Optical Antennas. *Phys. Rev. Lett.* **98,** 266802 (2007).

19. Genet, C. & Ebbesen, T. W. Light in tiny holes. *Nature* **445,** 39–46 (2007).

20. García de Abajo, F. J. Colloquium: Light scattering by particle and hole arrays. *Rev. Mod. Phys.* **79,** 1267–1290 (2007).

21. Parsons, J. *et al.* Localized surface-plasmon resonances in periodic nondiffracting metallic nanoparticle and nanohole arrays. *Phys. Rev. B* **79,** 073412 (2009).

22. Falcone, F. *et al.* Babinet principle applied to the design of metasurfaces and metamaterials. *Phys. Rev. Lett.* **93,** 197401 (2004).

23. Zentgraf, T. *et al.* Babinet's principle for optical metamaterials and nanoantennas. *Phys. Rev. B* **76,** 033407 (2007).

24. Ebbesen, T. W., Lezec, H. J., Ghaemi, H. F., Thio, T. & Wolff, P. A. Extraordinary optical transmission through sub-wavelength hole arrays. *Nature* **391,** 667–669 (1998).

25. Boltasseva, A. & Shalaev, V. M. Fabrication of optical negative-index metamaterials: recent advances and outlook. *Metamaterials* **2,** 1–17 (2008).

26. Rechberger, W. *et al.* Optical properties of two interacting gold nanoparticles. *Opt. Commun.* **220,** 137–141 (2003).

27. Prodan, E., Radloff, C., Halas, N. J. & Nordlander, P. A hybridization model for the plasmon response of complex nanostructures. *Science* **302,** 419–22 (2003).

28. Luk'yanchuk, B. *et al.* The Fano resonance in plasmonic nanostructures and metamaterials. *Nat. Mater.* **9,** 707–715 (2010).

29. Lovera, A., Gallinet, B., Nordlander, P. & Martin, O. J. F. Mechanisms of Fano Resonances in Coupled Plasmonic Systems. *ACS Nano* **7,** 4527–4536 (2013).

30. Dahmen, C., Schmidt, B. & von Plessen, G. Radiation damping in metal nanoparticle pairs. *Nano Lett.* **7,** 318–322 (2007).

31. Olk, P., Renger, J., Wenzel, M. T. & Eng, L. M. Distance dependent spectral tuning of two coupled metal nanoparticles. *Nano Lett.* **8,** 1174–1178 (2008).

32. Su, K.-H. *et al.* Interparticle Coupling Effects on Plasmon Resonances of Nanogold Particles. *Nano Lett.* **3,** 1087–1090 (2003).

33. Pinchuk, A. O. & Schatz, G. C. Nanoparticle optical properties: Far- and near-field electrodynamic coupling in a chain of silver spherical nanoparticles. *Mater. Sci. Eng. B* **149,** 251–258 (2008).

34. Decker, M., Feth, N., Soukoulis, C. M., Linden, S. & Wegener, M. Retarded long-range interaction in split-ring-resonator square arrays. *Phys. Rev. B* **84,** 085416 (2011).

35. Lunnemann, P., Sersic, I. & Koenderink, A. F. Optical properties of two-dimensional magnetoelectric point scattering lattices. *Phys. Rev. B* **88,** 245109 (2013).

36. Hendry, E., Mikhaylovskiy, R. V., Barron, L. D., Kadodwala, M. & Davis, T. J. Chiral Electromagnetic Fields Generated by Arrays of Nanoslits. *Nano Lett.* **12,** 3640–3644 (2012).

37. Schäferling, M., Dregely, D., Hentschel, M. & Giessen, H. Tailoring Enhanced Optical Chirality: Design Principles for Chiral Plasmonic Nanostructures. *Phys. Rev. X* **2,** 031010 (2012).

38. Meinzer, N., Hendry, E. & Barnes, W. L. Probing the chiral nature of electromagnetic fields surrounding plasmonic nanostructures. *Phys. Rev. B* **88,** 041407 (2013).

39. Hentschel, M., Schäferling, M., Weiss, T., Liu, N. & Giessen, H. Three-Dimensional Chiral Plasmonic Oligomers. *Nano Lett.* **12,** 2542–2547 (2012).

40. Plum, E., Fedotov, V. A., Schwanecke, A. S., Zheludev, N. I. & Chen, Y. Giant optical gyrotropy due to electromagnetic coupling. *Appl. Phys. Lett.* **90,** 223113 (2007).

41. Gansel, J. K. *et al.* Gold helix photonic metamaterial as broadband circular polarizer. *Science (80-.).* **325,** 1513–1515 (2009).

42. Decker, M., Zhao, R., Soukoulis, C. M., Linden, S. & Wegener, M. Twisted split-ring-resonator photonic metamaterial with huge optical activity. *Opt. Lett.* **35,** 1593–1595 (2010).

43. Hendry, E. *et al.* Ultrasensitive detection and characterization of biomolecules using superchiral fields. *Nat. Nanotechnol.* **5,** 783–787 (2010).

44. Shamonina, E., Kalinin, V. a., Ringhofer, K. H. & Solymar, L. Magnetoinductive waves in one, two, and three dimensions. *J. Appl. Phys.* **92,** 6252 (2002).

45. Weick, G., Woollacott, C., Barnes, W. L., Hess, O. & Mariani, E. Dirac-like Plasmons in Honeycomb Lattices of Metallic Nanoparticles. *Phys. Rev. Lett.* **110,** 106801 (2013).

46. Kravets, V. G., Schedin, F. & Grigorenko, A. N. Extremely Narrow Plasmon Resonances Based on Diffraction Coupling of Localized Plasmons in Arrays of Metallic Nanoparticles. *Phys. Rev. Lett.* **101,** 087403 (2008).

47. Chu, Y., Schonbrun, E., Yang, T. & Crozier, K. B. Experimental observation of narrow surface plasmon resonances in gold nanoparticle arrays. *Appl. Phys. Lett.* **93,** 181108 (2008).

48. Auguié, B. & Barnes, W. L. Collective Resonances in Gold Nanoparticle Arrays. *Phys. Rev. Lett.* **101,** 143902 (2008).

49. Vecchi, G., Giannini, V. & Gómez Rivas, J. Shaping the Fluorescent Emission by Lattice Resonances in Plasmonic Crystals of Nanoantennas. *Phys. Rev. Lett.* **102,** 146807 (2009).

50. Lozano, G. *et al.* Plasmonics for solid-state lighting: enhanced excitation and directional emission of highly efficient light sources. *Light Sci. Appl.* **2,** e66 (2013).

51. Lozano, G., Barten, T., Grzela, G. & Gómez Rivas, J. Directional absorption by phased arrays of plasmonic nanoantennae probed with time-reversed Fourier microscopy. *New J. Phys.* **16,** 013040 (2014).

52. Gallinet, B. & Martin, O. J. F. Refractive Index Sensing with Subradiant Modes : A Framework To Reduce Losses in Plasmonic Nanostructures. *ACS Nano* **7,** 6978–6987 (2013).

53. Fedotov, V. A., Rose, M., Prosvirnin, S. L., Papasimakis, N. & Zheludev, N. Sharp Trapped-Mode Resonances in Planar Metamaterials with a Broken Structural Symmetry. *Phys. Rev. Lett.* **99,** 147401 (2007).

54. Rodriguez, S. R. K. *et al.* Coupling Bright and Dark Plasmonic Lattice Resonances. *Phys. Rev. X* **1,** 021019 (2011).

55. Schokker, A. H. & Koenderink, A. F. Lasing at the band edges of plasmonic lattices. *sub to Phys Rev B* (2014).

56. Stehr, J. *et al.* A Low Threshold Polymer Laser Based on Metallic Nanoparticle Gratings. *Adv. Mater.* **15,** 1726–1729 (2003).

57. Zhou, W. *et al.* Lasing action in strongly coupled plasmonic nanocavity arrays. *Nat. Nanotechnol.* **8,** 506–511 (2013).

58. Van Exter, M. P. *et al.* Surface plasmon dispersion in metal hole array lasers. *Opt. Express* **21,** 27422–27437 (2013).

59. Van Beijnum, F. *et al.* Surface Plasmon Lasing Observed in Metal Hole Arrays. *Phys. Rev. Lett.* **110,** 206802 (2013).

60. Samuel, I. D. W., Namdas, E. B. & Turnbull, G. A. How to recognize lasing. *Nat. Photonics* **3,** 546–549 (2009).

61. Hill. ??? *This issue Nat. Photonics*

62. Zhou, W. & Odom, T. W. Tunable subradiant lattice plasmons by out-of-plane dipolar interactions. *Nat. Nanotechnol.* **6,** 423–427 (2011).

63. García de Abajo, F. J. Optical excitations in electron microscopy. *Rev. Mod. Phys.* **82,** 209–275 (2010).

64. Schmidt, F.-P. *et al.* Universal dispersion of surface plasmons in flat nanostructures. *Nat. Commun.* **5,** 3604 (2014).

65. Scholl, J. A., Koh, A. L. & Dionne, J. A. Quantum plasmon resonances of individual metallic nanoparticles. *Nature* **483,** 421–427 (2012).

66. Han, D., Lai, Y., Zi, J., Zhang, Z.-Q. & Chan, C. T. Dirac Spectra and Edge States in Honeycomb Plasmonic Lattices. *Phys. Rev. Lett.* **102,** 123904 (2009).

67. Novoselov, K. S. *et al.* Two-dimensional gas of massless Dirac fermions in graphene. *Nature* **438,** 197–200 (2005).

68. Zhang, Y., Tan, Y.-W., Stormer, H. L. & Kim, P. Experimental observation of the quantum Hall effect and Berry's phase in graphene. *Nature* **438,** 201–4 (2005).

69. Cheianov, V. & Fal'ko, V. Selective transmission of Dirac electrons and ballistic magnetoresistance of n-p junctions in graphene. *Phys. Rev. B* **74,** 041403 (2006).

70. Weick, G. & Mariani, E. Tunable plasmon polaritons in arrays of interacting metallic nanoparticles. Preprint at arXiv:1403.2205v1 (2014).

71. Balanis, C. A. *Antenna Theory: Analysis and Design*. (Wiley, 2005).

72. Pors, A., Nielsen, G. M., Eriksen, R. L. & Bozhevolnyi, S. I. Broadband focusing flat mirrors based on plasmonic gradient metasurfaces. *Nano Lett.* **13,** 829–834 (2013).

73. Pors, A. & Bozhevolnyi, S. I. Plasmonic metasurfaces for efficient phase control in reflection. *Opt. Express* **21,** 27438–27451 (2013).

74. Pozar, D. M., Targonski, S. D. & Syrigos, H. D. Design of Millimeter Wave Microstrip Reflectarrays. *IEEE Trans. Antennas Propag.* **45,** 287–296 (1997).

75. Sun, S. *et al.* Gradient-index meta-surfaces as a bridge linking propagating waves and surface waves. *Nat. Mater.* **11,** 426–431 (2012).

76. Walther, B. *et al.* Spatial and spectral light shaping with metamaterials. *Adv. Mater.* **24,** 6300–6304 (2012).

77. Chen, W. T. *et al.* High-efficiency broadband meta-hologram with polarization-controlled dual images. *Nano Lett.* **14,** 225–230 (2014).

78. Hu, D. *et al.* Ultrathin Terahertz Planar Elements. *Adv. Opt. Mater.* **1,** 186–191 (2013).

79. Ni, X., Kildishev, A. V & Shalaev, V. M. Metasurface holograms for visible light. *Nat. Commun.* **4,** 2807 (2013).

80. Yu, N. *et al.* Light Propagation with Phase Discontinuities: Generalized Laws of Reflection and Refraction. *Science (80-.).* **334,** 333–337 (2011).

81. Larouche, S. & Smith, D. R. Reconciliation of generalized refraction with diffraction theory. *Opt. Lett.* **37,** 2391–2393 (2012).

82. Magnusson, R. & Gaylord, T. K. Diffraction efficiencies of thin phase gratings with arbitrary grating shape. *J. Opt. Soc. Am.* **68,** 806–809 (1978).

83. Huang, L. *et al.* Dispersionless phase discontinuities for controlling light propagation. *Nano Lett.* **12,** 5750–5755 (2012).

84. Allen, L. & Beijersbergen, M. W. Orbital angular-momentum of light and the transformation of Laguerre-Gaussian laser modes. *Phys. Rev. A* **45,** 8185–8189 (1992).

85. Padgett, M., Courtial, J. & Allen, L. Light's orbital angular momentum. *Phys. Today* **57,** 35–40 (2004).

86. Yu, N. *et al.* A broadband, background-free quarter-wave plate based on plasmonic metasurfaces. *Nano Lett.* **12,** 6328–6333 (2012).

87. Aieta, F. *et al.* Aberration-free ultrathin flat lenses and axicons at telecom wavelengths based on plasmonic metasurfaces. *Nano Lett.* **12,** 4932–4936 (2012).

88. Chen, X. *et al.* Dual-polarity plasmonic metalens for visible light. *Nat. Commun.* **3,** 1198 (2012).

89. Huang, L. *et al.* Three-dimensional optical holography using a plasmonic metasurface. *Nat. Commun.* **4,** 2808 (2013).

90. Zhang, H., Tan, Q. & Jin, G. Holographic display system of a three-dimensional image with distortion-free magnification and zero-order elimination. *Opt. Eng.* **51,** 075801 (2012).

91. Avayu, O., Eisenbach, O., Ditcovski, R. & Ellenbogen, T. Optical metasurfaces for polarization-controlled beam shaping. *Opt. Lett.* **39,** 3892–3895 (2014).

92. Yu, N. & Capasso, F. Flat optics with designer metasurfaces. *Nat. Mater.* **13,** 139–150 (2014).

93. Onoda, M., Murakami, S. & Nagaosa, N. Hall Effect of Light. *Phys. Rev. Lett.* **93,** 083901 (2004).

94. Yin, X., Ye, Z., Rho, J., Wang, Y. & Zhang, X. Photonic spin Hall effect at metasurfaces. *Science (80-.).* **339,** 1405–1407 (2013).

95. Hirsch, J. E. Spin Hall Effect. *Phys. Rev. Lett.* **83,** 1834–1837 (1999).

96. Zou, L. *et al.* Dielectric resonator nanoantennas at visible frequencies. *Opt. Express* **21,** 1344–52 (2013).

97. Decker, M. *et al.* High-efficiency light-wave control with all-dielectric optical Huygens' metasurfaces. arXiv:1405.5038v1 (2014).

98. Dal Negro, L. & Boriskina, S. V. Deterministic aperiodic nanostructures for photonics and plasmonics applications. *Laser Photon. Rev.* **6,** 178–218 (2012).

99. Wiersma, D. S. Random Lasers Explained. *Nat. Photonics* **3,** 246–248 (2009).

100. Leonetti, M., Conti, C. & Lopez, C. The mode-locking transition of random lasers. *Nat. Photonics* **5,** 615–617 (2011).

101. Zheludev, N. I., Prosvirnin, S. L., Papasimakis, N. & Fedotov, V. A. Lasing spaser. *Nat. Photonics* **2,** 351–354 (2008).

102. Armelles, G., Cebollada, A., García-Martín, A. & González, M. U. Magnetoplasmonics: Combining Magnetic and Plasmonic Functionalities. *Adv. Opt. Mater.* **1,** 10–35 (2013).

103. Lee, J. *et al.* Giant nonlinear response from plasmonic metasurfaces coupled to intersubband transitions. *Nature* **511,** 65–69 (2014).

104. Torma, P. & Barnes, W. L. Strong coupling between surface plasmon polaritons and emitters. *Reports Prog. Phys.* **in-press,** (2014).

105. Zengin, G. *et al.* Approaching the strong coupling limit in single plasmonic nanorods interacting with J-aggregates. *Sci. Rep.* **3,** 3074 (2013).

106. Väkeväinen, A. I. *et al.* Plasmonic surface lattice resonances at the strong coupling regime. *Nano Lett.* **14,** 1721–1727 (2014).

107. Zhang, Y., Lu, F., Yager, K. G., van der Lelie, D. & Gang, O. A general strategy for the DNA-mediated self-assembly of functional nanoparticles into heterogeneous systems. *Nat. Nanotechnol.* **8,** 865–72 (2013).

108. Decker, M., Klein, M. W., Wegener, M. & Linden, S. Circular dichroism of planar chiral magnetic metamaterials. *Opt. Lett.* **32,** 856–858 (2007).

109. Gwinner, M. C. *et al.* Periodic large-area metallic split-ring resonator metamaterial fabrication based on shadow nanosphere lithography. *Small* **5,** 400–406 (2009).

110. Nikolaenko, A. E. *et al.* Carbon Nanotubes in a Photonic Metamaterial. *Phys. Rev. Lett.* **104,** 153902 (2010).

111. Wu, W. *et al.* Optical metamaterials at near and mid-IR range fabricated by nanoimprint lithography. *Appl. Phys. A* **87,** 143–150 (2007).

112. Yu, N. *et al.* Flat Optics: Controlling Wavefronts With Optical Antenna Metasurfaces. *IEEE J. Sel. Top. Quantum Electron.* **19,** 4700423–4700423 (2013).

113. Padilla, W. J., Basov, D. N. & Smith, D. R. Negative refractive index metamaterials. *Mater. Today* **9,** 28–35 (2006).

114. Shalaev, V. M. Optical negative-index metamaterials. *Nat. Photonics* **1,** 41–48 (2007).

115. Soukoulis, C. M., Linden, S. & Wegener, M. Negative Refractive Index at Optical Wavelengths. *Science (80-.).* **315,** 47–49 (2007).

116. Liu, L. *et al.* Broadband Metasurfaces with Simultaneous Control of Phase and Amplitude. *Adv. Mater.* **26,** 5031–5036 (2014).

117. Pendry, J. B., Holden, A. J., Robbins, D. J. & Stewart, W. J. Magnetism from conductors and enhanced nonlinear phenomena. *IEEE Trans. Microw. Theory Tech.* **47,** 2075–2084 (1999).

118. Smith, D. . R., Padilla, W. J., Vier, D. C., Nemat-Nasser, S. C. & Schultz, S. Composite medium with simultaneously negative permeability and permittivity. *Phys. Rev. Lett.* **84,** 4184–4187 (2000).

119. Linden, S. *et al.* Magnetic response of metamaterials at 100 terahertz. *Science* **306,** 1351–1353 (2004).

120. Husnik, M. *et al.* Absolute extinction cross-section of individual magnetic split-ring resonators. *Nat. Photonics* **2,** 614–617 (2008).

121. Zhang, S. *et al.* Experimental Demonstration of Near-Infrared Negative-Index Metamaterials. *Phys. Rev. Lett.* **95,** 137404 (2005).

122. Kats, M. A. *et al.* Giant birefringence in optical antenna arrays with widely tailorable optical anisotropy. *Proc. Natl. Acad. Sci.* **109,** 12364–12368 (2012).

123. Pancharatnam, S. Generalized theory of interference, and its applications. Part 1. Coherent Pencils. *Proc. Indian Acad. Sci. A* **44,** 247–262 (1956).

124. Berry, M. V. The adiabatic phase and pancharatnam's phase for polarized light. *J. Mod. Opt.* **34,** 1401–1407 (1987).

125. Bomzon, Z., Kleiner, V. & Hasman, E. Pancharatnam--Berry phase in space-variant polarization-state manipulations with subwavelength gratings. *Opt. Lett.* **26,** 1424–1426 (2001).